Separation Science and Technology
Publication details, including instructions for authors and subscription information:
http://www.informaworld.com/smpp/title~content=t713708471

A Theoretical Model for Bubble Formation at a Frit Surface in a Shear Field

Bruce D. Johnson[a]; Robert M. Gershey[a]; Robert C. Cooke[a]; William H. Sutcliffe Jr.[b]
[a] DEPARTMENT OF OCEANOGRAPHY, DALHOUSIE UNIVERSITY HALIFAX, NOVA SCOTIA, CANADA [b] DEPARTMENT OF FISHERIES AND OCEANS BEDFORD, INSTITUTE OF OCEANOGRAPHY DARTMOUTH, NOVA SCOTIA, CANADA

To cite this Article Johnson, Bruce D. , Gershey, Robert M. , Cooke, Robert C. and Sutcliffe Jr., William H.(1982) 'A Theoretical Model for Bubble Formation at a Frit Surface in a Shear Field', Separation Science and Technology, 17: 8, 1027 — 1039
To link to this Article: DOI: 10.1080/01496398208060267
URL: http://dx.doi.org/10.1080/01496398208060267

SEPARATION SCIENCE AND TECHNOLOGY, 17(8), pp. 1027–1039, 1982

A Theoretical Model for Bubble Formation at a Frit Surface in a Shear Field

BRUCE D. JOHNSON, ROBERT M. GERSHEY, and ROBERT C. COOKE

DEPARTMENT OF OCEANOGRAPHY
DALHOUSIE UNIVERSITY
HALIFAX, NOVA SCOTIA, CANADA B3H 4J1

WILLIAM H. SUTCLIFFE, JR.

DEPARTMENT OF FISHERIES AND OCEANS
BEDFORD INSTITUTE OF OCEANOGRAPHY
DARTMOUTH, NOVA SCOTIA, CANADA B2Y 4A2

Abstract

Engineers, meteorologists, and oceanographers all have an interest in the behavior of small air bubbles in water. Studies that are concerned with the separation of dissolved and particulate species, aerosol formation, and oceanic particle production require a means for the generation of large numbers of small bubbles. A device that produces populations of small bubbles (between 15 and 100 μm in radius) with predictable size distributions has been developed and is described. A model based upon an analysis of the form drag on a bubble emerging from a submerged orifice in a shear field successfully predicts the number-size distribution of bubbles produced by the bubble generator.

INTRODUCTION

The significance of bubble size has been demonstrated empirically or theoretically in a number of studies involving separations of dissolved and particulate substances relevant to industrial and water treatment processes; e.g., Cassel et al. (*7*), DeVivo and Karger (*9*), and Flint and Howarth (*10*). Similarly, bubble size has been shown to be an important parameter in studies of processes of oceanographic and marine atmospheric importance (*2, 4, 5, 12*). In industrial processes, enhanced separation efficiencies are sought, while in seawater studies, effects related to bubble size must be examined in the context of observed marine bubble populations. Bubbles in

the ocean have been found to range in size from a few micrometers (*13*) to centimeters (*8*), with a large proportion of the bubbles produced by a breaking wave being less than 100 μm in radius (*6*).

Although bubble size is generally recognized to be an important variable in seawater bubbling studies, many such studies have employed bubbles of poorly defined size distribution and with sizes uncharacteristic of oceanic populations. This is no doubt because there are few methods of producing bubbles of predictable size distribution. This is especially true for small (less than about 500 μm) bubbles.

Populations of bubbles are usually produced in bubbling studies by forcing air through sintered glass frits or dispersers. However, sizes of bubbles produced in this manner typically exceed 200 μm in radius, and size distributions must be determined photographically or by some other means. For the removal of impurities from water and wastewater by microflotation, small bubbles are produced with frits by the addition of alcohols (frothing agents); e.g., Cassel et al. (*7*). This procedure does permit production of bubbles as small as 25 μm, but the presence of the alcohol introduces a variable that must be considered when interpreting the results and is not a practical approach for producing small bubbles in seawater. Likewise, the electrolytical production of small bubbles changes the seawater chemistry. Blanchard and Syzdek (*5*) developed a method for producing single bubbles as small as 10 μm in radius with impressive reproducibility, but while this method is ideal for examining single bubble dynamics, a method of producing large numbers of small bubbles is desirable for certain experimental designs.

Because of the necessity of producing populations of bubbles of less than 200 μm in radius for studies of the effects of bubbles in seawater, a purely physical method was developed that possesses the added advantage of allowing the bubble number–size distribution to be determined *a priori* from theoretical considerations.

THEORY

Blanchard's (*3*) analysis of the production of small bubbles by capillaries, equally applicable to frits, reveals the nature of the forces involved. As he concluded, a bubble is released when, "... the bubble buoyancy force equals the surface tension force that holds the bubble on the tip." In order to produce small bubbles to examine enrichment of bacteria in jet drops, Blanchard and Syzdek (*5*) immersed the tip of a capillary in a rotating tank of water and thus utilized drag forces instead of buoyancy forces to overcome the forces due to surface tension. Similarly, drag forces can be utilized to produce large numbers of small bubbles with a frit. However, instead of using

the rotating tank arrangement described by Blanchard and Syzdek, the fluid boundary layer that develops in flow along the surface of a frit was effectively controlled by restricting water flow to a narrow channel adjacent to the frit surface. After some analysis of the significant variables, the apparatus shown in Fig. 1 was assembled.

In this apparatus a glass disk is maintained in position above the surface of a frit of the same diameter by a glass tube passing through the hole in the disk center. An O-ring in contact with a beaded region of the tube eliminates leaks while providing a small positive force to hold the disk against the frit. To maintain the relative positions of the frit and disk, the frit inlet tube is bent 180° into a position parallel to the disk inlet tube, and two glass tie rods are positioned in the gap.

In operation, water pumped through the tube in the center of the disk produces a separation of disk and frit, and flows radially outward along the frit surface. Bubbles emerging from the frit are subjected to drag forces and are separated from the frit at sizes much smaller than would be the case if buoyancy were the only force operating.

With some simplifying assumptions, a model can be developed to predict bubble size as a function of water flow rate and disk and frit separation. The assumptions include:

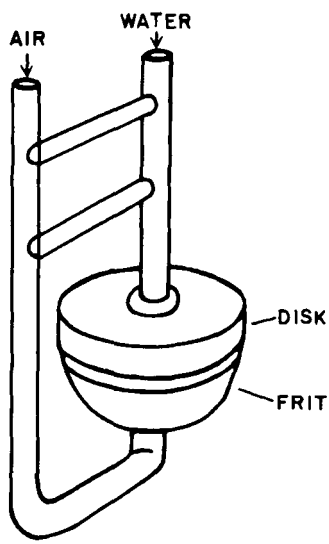

FIG. 1. Frit and disk bubble generator.

1. The flow between the frit and disk is laminar and is fully developed over the entire frit surface.
2. Bubbles emerging from the frit pores experience significant force only from drag.
3. The gas to water flow rate ratio is sufficiently small that the effects of coalescence are negligible and the properties of the fluid remain those of the entering water.
4. Fluid flow streamlines are not affected by interactions with bubbles upstream or affected by surface roughness of the frit. (To reduce surface roughness, the bubble-producing surface of the frit was polished before use with 400-grit waterproof abrasive paper.)

Under these conditions, separation of the bubble at the frit occurs when a bubble radius is reached such that drag forces on the bubble equal the surface tension force $\pi D\gamma$:

$$C_{D'} \frac{\rho U_0^2 A_p}{2} = \pi D\gamma \tag{1}$$

where ρ is the fluid density, U_0 is the fluid velocity, A_p is the projected bubble area, γ is the gas-water surface tension, and D is the pore diameter of the frit. The significance of $C_{D'}$, a constant analogous to the drag coefficient, will be discussed in a later section. Because of the assumption of developed flow, the velocity varies across the fluid stream from zero at the frit and disk surfaces to a maximum at $S/2$, where S is the separation between the disk and frit. Thus, in the evaluation of the drag on an emerging bubble, the square of the velocity as a function of position relative to the frit surface must be integrated over the projected area of the bubble.

Batchelor (*1*) presents an equation in two dimensions that describes fluid velocity, U, under a pressure gradient, G, between two fixed and rigid planes:

$$U = \frac{G}{2\mu}(yS - y^2) \tag{2}$$

where μ is the viscosity and y is the distance from one plane, in this case, the frit surface. The average velocity can be determined by integrating the velocity, U, over S and dividing by S,

$$U_{avg} = \frac{2}{S}\int_0^{S/2} \frac{S^2 G}{8\mu}\left[\frac{4y}{S} - \frac{4y^2}{S^2}\right] dy \tag{3}$$

yielding

$$U_{avg} = S^2 G/12\mu \tag{4}$$

Comparing U_{avg} to U_{max} gives

$$U_{max} = 1.5 U_{avg} \tag{5}$$

Here U_{avg} is merely

$$U_{avg} = U_{vol}/(2\pi LS) \tag{6}$$

where U_{vol} is the volume flow rate of water, a known quantity, and L is the radial frit position. Thus the local velocity as a function of volume flow rate between the frit and disk is

$$U = \frac{3}{4\pi LS} U_{vol} \left[\frac{4y}{S} - \frac{4y^2}{S^2} \right] \tag{7}$$

For a single bubble emerging from the frit, the result of U^2 integrated over the projected bubble area can be found by converting to cylindrical coordinates, viz.,

$$U_0^2 A_p = 2 \int_0^{\pi/2} \int_0^{2R\cos\theta} \left[\frac{3}{4\pi LS} U_{vol} \right]^2 \times \left[\frac{16r^2}{S^2} \cos^2\theta - \frac{32r^3}{S} \cos^3\theta + \frac{16r^4}{S^4} \cos^4\theta \right] r\, dr\, d\theta \tag{8}$$

with U_0 being the area-weighted mean velocity, R being the bubble radius, and r being the distance from the axis center at the surface of the frit. Integration yields

$$U_0^2 A_p = \frac{U_{vol}^2 R^4}{2L^2 S^4 \pi} \left[\frac{45}{2} - 63\frac{R}{S} + \frac{189}{4} \frac{R^2}{S^2} \right] \tag{9}$$

and the drag on an emerging bubble is then

$$F_d = C_D \rho \left[\frac{U_{vol}^2 R^4}{4L^2 S^4 \pi} \right] \left[\frac{45}{2} - 63\frac{R}{S} + \frac{189}{4} \frac{R^2}{S^2} \right] \tag{10}$$

Bubble separation occurs when

$$C_{D'}\rho\left[\frac{U_{\text{vol}}^2R^4}{4L^2S^4\pi}\right]\left[\frac{45}{2}-63\frac{R}{S}+\frac{189}{4}\frac{R^2}{S^2}\right]=\pi D\gamma \quad (11)$$

Thus a bubble is swept from the frit when a radius is reached such that the dynamic separating force due to drag equals the retention force due to surface tension.

If it is assumed that the gas flow rate is constant over the frit surface, the rate of bubble generation, N, as a function of radial frit position and total gas flow rate, W, can be determined by the expression

$$N=\frac{3}{\pi R^3}\int_{L_1}^{L_2}\int_0^{\pi/2}\int_0^{W/(\pi L_w^2)}dz\,d\theta\,L\,dL \quad (12)$$

or

$$N=\int_{L_1}^{L_2}\frac{3WL}{2\pi R^3L_w^2}dL \quad (13)$$

where L_w is the radius of the bubble generating surface of the frit, z is the axis at the frit center normal to the plane of the frit surface, and R is the radius of bubble at separation for position L on the frit. However, from (11),

$$L=\left[\frac{C_{D'}\rho U_{\text{vol}}^2R^4}{4S^4\pi^2D\gamma}\left[\frac{45}{2}-63\frac{R}{S}+\frac{189}{4}\frac{R^2}{S^2}\right]\right]^{1/2} \quad (14)$$

and thus N can be expressed in terms of R alone as

$$N=\frac{3C_{D'}\rho U_{\text{vol}}^2W}{8L_w^2S^4\pi^3D\gamma}\int_{R_1}^{R_2}45-\frac{315}{2}\frac{R}{S}+\frac{567}{4}\frac{R^2}{S^2}dR \quad (15)$$

The result of this integral is

$$N=\frac{3C_{D'}\rho U_{\text{vol}}^2W}{8L_w^2S^4\pi^3D\gamma}\left[45R-\frac{315}{4}\frac{R^2}{S}+\frac{567}{12}\frac{R^3}{S^2}\right]_{R_1}^{R_2} \quad (16)$$

The significance of $C_{D'}$ for bubble separation from the frit can be

determined through combination of Eq. (1) with a dimensionless parameter that describes the relative importance of inertial and viscous forces.

$$C_{D'} = \frac{2\pi D\gamma}{A_p \rho U_0^2} \quad \text{and} \quad \frac{2RU_0}{\nu} \tag{17}$$

where ν is the kinematic viscosity, and from which

$$C_{D'}\left[\frac{2RU_0}{\nu}\right]^2 = \frac{8D\gamma}{\rho\nu^2} \tag{18}$$

Here $(2RU_0)/\nu$ is analogous to the Reynolds number. Since ν, γ, and ρ are properties of the water and D, the frit pore diameter, is known within narrow limits, the value of $(8D\gamma/\rho\nu^2)$ is constant. A plot of $C_{D'}$ vs $(2RU_0/\nu)$ for this fixed value of $(8D\gamma/\rho\nu^2)$ then describes a line for which the separation force is constant. The intersection of this line with an empirically determined resistance curve for a bubble immersed in a flow field will determine the unique value of $C_{D'}$, which is independent of frit geometry, bubble size, and water velocity.

Bubbles exhibit a range of resistance curves as a result of their differing surface mobilities (*16*). Consequently, the exact value of $C_{D'}$ cannot be predicted. However, the limits on $C_{D'}$ can be determined as the points of intersection of the line of constant force with the resistance curves for bubbles that exhibit fluid sphere and solid sphere behavior, and are 0.5 and 2.0, respectively.

Thus for a given separation of frit and disk, and for a given volume flow rate of water, the size range of bubbles produced by the bubble generating apparatus can be caluclated from Eq. (11). Equation (16) can then be utilized to determine the numbers of bubbles generated from the known bubble size range, or for any part of that range.

EXPERIMENTAL

Seawater was pumped with a peristaltic pump from a reservoir, passed through a partially filled 2-L round-bottomed flask to damp surges, and introduced into the disk-center tube of the bubble generator. Gas (helium in this case, although the type of gas is largely immaterial) was introduced into the glass tube leading to a 3.2-cm diameter glass frit of 4.0–5.5 μm pore size. Before each experiment the water flow rate was measured by holding the bubble generator over a volumetric flask and noting the time required for

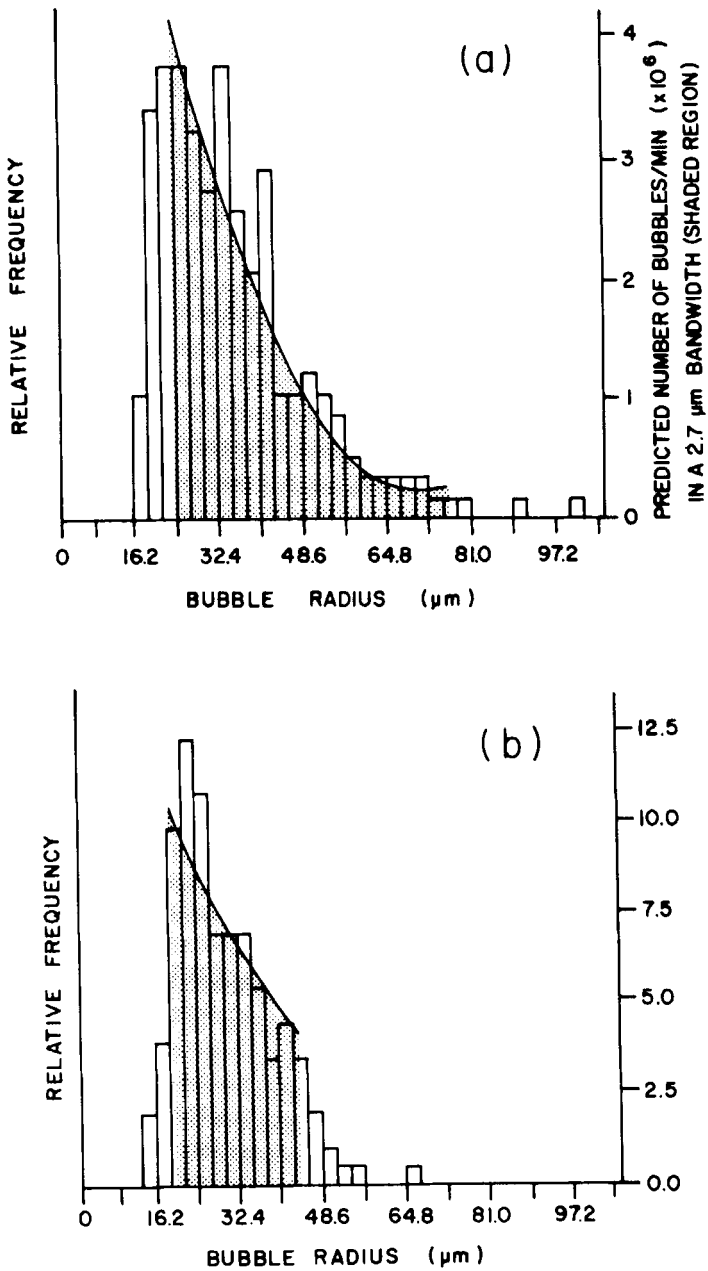

FIG. 2. Bubble distributions produced by the frit and disk generator with gas flow rates of 8 cm^3/min and water flow rates of (a) 243 cm^3/min, (b) 500 cm^3/min, and (c) 776 cm^3/min.

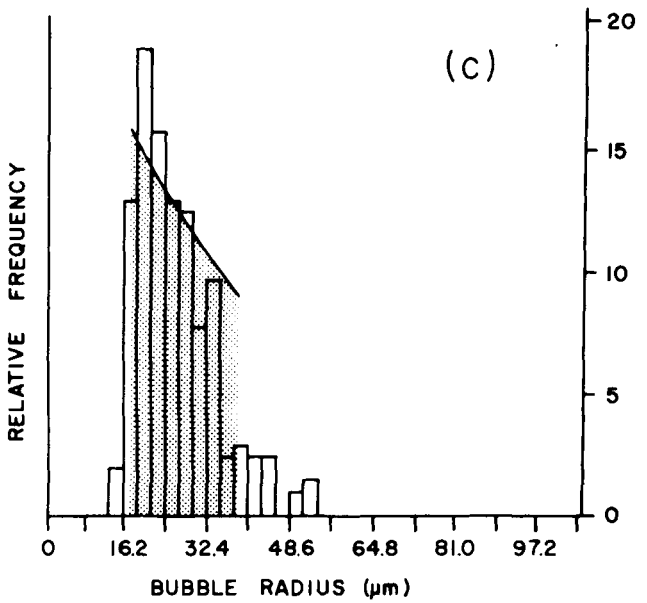

filling. The gas flow rate was found by maintaining the bubble generator in a water reservoir and determining the rate of water displacement by the gas in an inverted water-filled beaker. Because the flow-induced separation of disk and frit varied according to flow rate, the separation was measured with calibrated shim stock under the conditions of flow for each experiment.

At the beginning of each experiment the bubble generator was operated for several minutes in a beaker of seawater to insure a steady state. The generator was then introduced into a reservoir of seawater in which there was a seawater-filled Plexiglas cell similar to that described by Cipriano and Blanchard (*8*). This Plexiglas cell of 1 × 6 cm rectangular cross section was inverted with its open end slightly below the reservoir surface while the main portion, sealed at the upper end, protruded above the air–water interface. The generator attitude was maintained such that emerging bubbles were injected directly into the seawater-filled cell, and photographs were made of a region very near the point of emergence of bubbles from the generator to insure that the source population, and not an aged population, was being photographed. Illumination was provided by strobe lamps facing the three accessible edges of the cell. The lens magnification was 0.5× and the film and method of development used are those described by Johnson and Cooke (*11*). Bubble images were measured directly from the film by microscope with the aid of an ocular micrometer. From 200 to 400 bubbles were

measured per distribution. Using this procedure, bubbles as small as 12 μm in radius were measurable.

RESULTS AND DISCUSSION

The distribution of bubbles produced by the generator with a gas flow rate of 8 cm^3/min and water flow rates of 243, 500, and 776 cm^3/min appear in the histograms of Figs. 2a–c, respectively. As can be seen in these distributions, virtually all of the bubbles produced under the flow conditions described are less than 100 μm in radius with a lower limit of about 15 μm and a range that narrows with increasing water flow rate. In the narrowest distribution, that for 776 cm^3/min water flow, the range is represented by radii of about 15 to 50 μm, with an average radius of only 25 μm.

Included in Fig. 2 are the ranges of size and the shapes of the distributions that are predicted by Eqs. (11) and (16) using a value of unity for $C_{D'}$. The size ranges and number distributions predicted by the model are seen to be quite good, with only a small fraction of the bubbles in any of the distributions falling outside of the predicted range. As Eq. (18) predicts, a single value of $C_{D'}$ seems to apply over the wide range of water flow rates and bubble sizes found in these experiments. However, the sensitivity of the model to the value of $C_{D'}$ is such that over the range of 0.5 to 1.5, the predictions of the model do not significantly change.

The validity of the assumptions upon which the model is based can be examined. The Reynolds number of the channel, SU_{avg}/ν, has a minimum of abour 40, which corresponds to the water flow rate of 243 cm^3/min at the edge of the frit. A maximum Reynolds number of about 500 is appropriate for the water flow rate at the center of the disk (776 cm^3/min). Thus, if 2100 represents the value of the Reynolds number above which transition to turbulent flow occurs, the flow conditions present in the bubble generator are well within the limits of the laminar regime.

The equation describing the development of flow between two flat plates (*15*) can be used to examine the assumption that developed flow over the region between the frit and disk exists. According to Schlichting, the flow is nearly fully developed when

$$L/S = 0.04N_{Re} \tag{19}$$

For the case of the bubble generator used in this work, L is the distance from the center of the frit and S is the separation of the frit and disk. For a Reynolds number of 500, the calculated value of L is 0.35 cm. This solution describes nearly fully developed flow, that is, where the boundary layer thickness is nearly equal to $S/2$. Bubbles in the transition region (i.e., at

distances of less than 0.35 cm from the center of the frit) are sheared from the frit at diameters that correspond to a vertical dimension which is closer to $S/5$. Thus for bubbles in this region, the flow is effectively developed at distances much less than 0.35 cm from the center of the frit. While the fluid velocity profile in the transition region is not exactly that of developed flow, the assumption of developed flow over the entire frit surface is a reasonable approximation.

The best proof of the validity of the assumptions made in developing Eqs. (11) and (16) lies in the fit of the data to the predicted number-size distribution at air flow rates of 8 cm^3/min. At higher ratios of gas flow to water flow, however, other factors seem to become important as demonstrated for a gas flow of 41 cm^3/min (Fig. 3). The absence of a term for the gas flow rate in Eq. (11) means that the size ranges of the distributions produced at a gas flow rate of 41 cm^3/min should, at about the same water flow rates, be nearly the same as those in Figs. 2a–c for the lower gas flow rate of 8 cm^3/min. This is obviously not true, with a greater number of large bubbles being produced at the higher gas flow rate. Marmur and Rubin (*14*) have described the effect of radial motion of the liquid on bubble formation at a submerged orifice. Above critical gas flow rates, bubble expansion due to

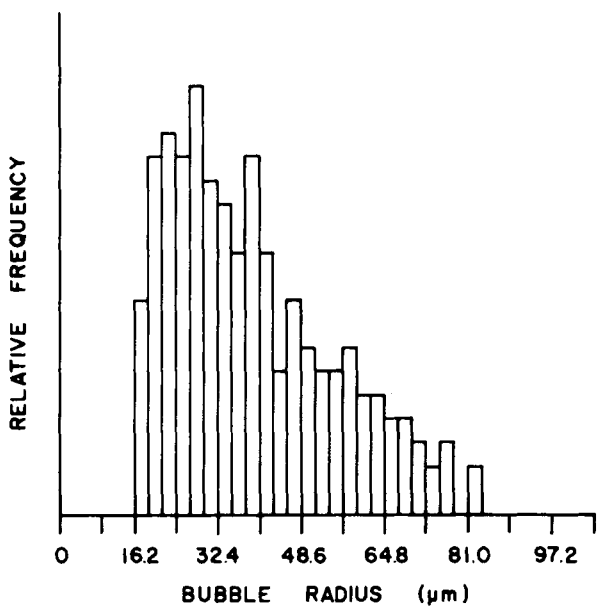

FIG. 3. Bubble distribution produced by the frit and disk generator with a gas flow rate of 41 cm^3/min and a water flow rate of 776 cm^3/min.

liquid inertia tends to make the bubbles larger than is predicted by models that ignore this inertial effect. In addition, higher gas flow rates cause the physical distance between bubbles to diminish, and a growing bubble may be retarded in its detachment by the close proximity of the preceding one. The present model does not consider mutual bubble interaction and would thus tend to predict smaller bubble sizes than those observed. If the flow rates were sufficiently high, one might also expect larger bubbles to be produced as a result of coalescence.

The assumption of constant gas flow over the frit surface appears to be justified judging from the fit of the model to the data. However, the apparent roughness of the observed bubble distributions could be the result of local variations in gas flow over the frit surface, although this appears to occur to a minor extent only.

CONCLUSIONS

Bubbles with sizes typical of those reported for oceanic populations are of greatest interest in studies of particle scavenging by rising bubbles and aerosol formation from bursting bubbles. The failure to consider bubble size in many such studies in the past has been due primarily to the absence of a method for producing populations of bubbles less than 100 μm in radius. Such a method is described here, and consists of an apparatus so constructed that bubbles emerging from a frit are sheared by water flow restricted to a narrow channel. Bubble populations produced in this manner typically have mean sizes smaller than 100 μm in radius.

A model which predicts the radius of an emerging bubble by equating the drag forces resulting from fluid flow to the surface tension force holding the bubble to the frit provides a very good description of the observed bubble populations. Within the limits of the assumptions of this model, bubble generators can be assembled that will produce a desired population of small bubbles of predetermined number and range. Although useful populations of small bubbles can be produced outside the limits of validity of the model, the parameters describing such populations must be determined empirically.

SYMBOLS

A_p	projected area of bubble
$C_{D'}$	drag constant
D	diameter of frit pore
F_D	drag force
G	pressure gradient
L	distance from center of frit
L_W	radius of frit

N	rate of bubble production
N_{Re}	Reynolds number
R	radius of bubble
r	distance from surface of frit
S	separation of frit and disk
U	local velocity
U_{avg}	average velocity
U_{max}	maximum velocity
U_0	area-weighted mean velocity
U_{vol}	volume flow rate
W	gas flow rate
y	distance from plane surface
z	axis normal to surface of frit
γ	gas–water surface tension
μ	dynamic viscosity
ν	kinematic viscosity
ρ	fluid density

Acknowledgment

This research was performed under contract number 08SC.FP806-9-0009 Fisheries and Oceans, Canada.

REFERENCES

1. G. K. Batchelor, *An Introduction to Fluid Dynamics*, Cambridge University Press, Cambridge, England, 1967, pp. 183–234.
2. D. C. Blanchard, "The Electrification of the Atmosphere by Particles from Bubbles in the Sea," *Prog. Oceanogr., 1*, 71–202 (1963).
3. D. C. Blanchard, *Chem. Eng. Sci., 32*, 1109 (1977).
4. D. C. Blanchard, *Pageoph., 116*, 302 (1978).
5. D. C. Blanchard and L. D. Syzdek, *J. Geophys. Res., 77*, 5087 (1972).
6. D. C. Blanchard and A. H. Woodcock, *Tellus, 9*, 145 (1957).
7. E. A. Cassel, K. M. Kaufman, and E. Matijevic, *Water Res., 9*, 1017 (1975).
8. R. Cipriano and D. C. Blanchard, *J. Geophys. Res., 86*, 8085 (1981).
9. D. G. DeVivo and B. L. Karger, *Sep. Sci., 5*, 145 (1970).
10. L. R. Flint and W. J. Howarth, *Chem. Eng. Sci., 26*, 1155 (1971).
11. B. D. Johnson and R. C. Cooke, *J. Geophys. Res., 84*, 3761 (1979).
12. B. D. Johnson and R. C. Cooke, *Limnol. Oceanogr., 25*, 653 (1980).
13. B. D. Johnson and R. C. Cooke, *Science, 213*, 209 (1981).
14. A. Marmur and E. Rubin, *Chem. Eng. Sci., 31*, 453 (1976).
15. H. Schlichting, *Boundary-Layer Theory*, McGraw-Hill, New York, 1968, p. 85.
16. R. Tedesco and D. C. Blanchard, *J. Rech. Atmos., 13*, 215 (1979).

Received by editor December 7, 1981